physica **pss** status solidi **b**

www.pss-b.com

*basic solid state physics*

# Environmental influence on linear optical spectra and relaxation dynamics in carbon nanotubes

**Ermin Malić*,[1], Matthias Hirtschulz[1], Janina Maultzsch[2], Stephanie Reich[3], and Andreas Knorr[1]**

[1] Institut für Theoretische Physik, Technische Universität Berlin, 10623 Berlin, Germany
[2] Institut für Festkörperphysik, Technische Universität Berlin, 10623 Berlin, Germany
[3] Fachbereich Physik, Freie Universität Berlin, 14195 Berlin, Germany

* Corresponding author: e-mail ermin@itp.physik.tu-berlin.de, Phone: +49-30-31423764, Fax: +49-30-314-21130

We present theoretical investigations on linear optical spectra and the temporal non-equilibrium dynamics of single-walled carbon nanotubes. In particular we discuss the importance of the surrounding medium. Our approach is based on the density matrix theory, which in combination with tight-binding wave functions allows the calculation of linear and nonlinear optical properties of arbitrary nanotubes. Its strength lies in the straightforward way to describe non-equilibrium properties, such as Coulomb driven ultrafast intrasubband carrier relaxation. We find a strong influence of the surrounding dielectric medium on the position of the peaks, the excitonic binding energy, and the carrier relaxation time. Furthermore, simple scaling laws describing the dependence on the dielectric background constant $\varepsilon_{\mathrm{bg}}$ are shown.

**1 Introduction** Optical properties of single-walled carbon nanotubes (CNTs) have been in focus of research since their discovery in the 1990s [1, 2]. The variety of CNTs exhibiting different chiral angles and diameters requires strategies to unambiguously characterize specific tube types in a sample containing thousands of different CNTs. Since nanotubes as one-dimensional structures show well-defined optical transitions, optical spectroscopy methods, such as absorption, photoluminescence, or Rayleigh scattering [3–6], can be exploited for characterization of CNTs. For investigation of characteristic features in optical spectra, it is important to take the influence of the surrounding medium into account. The environment created by solvents and adsorbed molecules has a considerable influence on the optical properties of CNTs [7–12]. It has an effect on both the transition energies as well as on the excitonic binding energy. The dependence on the environment offers a possibility to tailor the band gap of a nanotube by changing its surrounding medium. However, the creation of adjustable environments is still a challenge in current research.

In this work, we present excitonic absorption spectra and discuss the influence of the surrounding medium by including the dielectric background constant $\varepsilon_{\mathrm{bg}}$ into our calculations. We find fit functions describing the dependence of the excitation energy and the excitonic binding energy on $\varepsilon_{\mathrm{bg}}$. Furthermore, we have performed microscopic calculations of the ultrafast relaxation dynamics of optically excited electrons in CNTs. We focus on Coulomb driven scattering processes, which are found to lead to relaxation times of hot electrons on the femtosecond time scale depending on the population density and the dielectric background constant $\varepsilon_{\mathrm{bg}}$.

**2 Theoretical approach** Our goal is the microscopic description of (i) the temporal dynamics of the occupation probability $\rho_{\boldsymbol{k}}^{\lambda\lambda}(t) = \langle a_{\lambda\boldsymbol{k}}^{+} a_{\lambda\boldsymbol{k}} \rangle(t)$ in the state $|\lambda\boldsymbol{k}\rangle$ with the band index $\lambda$ and the wave vector $\boldsymbol{k}$, and (ii) the microscopic polarization $p_{\boldsymbol{k}}(t) \equiv \rho_{\boldsymbol{k}}^{\lambda\lambda'}(t) = \langle a_{\lambda\boldsymbol{k}}^{+} a_{\lambda'\boldsymbol{k}} \rangle(t)$, which is a measure for the transition probability between the two states $|\lambda\boldsymbol{k}\rangle$ and $|\lambda'\boldsymbol{k}\rangle$ [13]. Here, $a_{\lambda\boldsymbol{k}}$ and $a_{\lambda\boldsymbol{k}}^{+}$ are the annihilation and the creation operators, respectively, acting on an electron in the state $|\lambda\boldsymbol{k}\rangle$. The knowledge of $p_{\boldsymbol{k}}(t)$ and $\rho_{\boldsymbol{k}}^{\lambda\lambda}(t)$ allows the calculation of the absorption coefficient $\alpha(\omega) \propto \omega \operatorname{Im} \chi(\omega)$, since in the linear regime the optical susceptibility $\chi(\omega)$ can be expressed as a function of the microscopic polarization

WILEY InterScience®
DISCOVER SOMETHING GREAT

Phys. Status Solidi B **246**, No. 11–12 (2009)

2593

$p_{\boldsymbol{k}}(t)$ and the optical matrix element $\boldsymbol{M}(\boldsymbol{k})$ [14]:

$$\mathrm{Im}\,\chi(\omega) = -\frac{2e_0\hbar}{m_0\varepsilon_0\omega^2 A(\omega)}\sum_{\boldsymbol{k}}\mathrm{Re}(\boldsymbol{M}_z(\boldsymbol{k})p_{\boldsymbol{k}}(\omega)), \quad (1)$$

with the vector potential $A(\omega)$, the electron mass $m_0$, and the elementary charge $e_0$. The $z$-component of the optical matrix element $\boldsymbol{M}_z(\boldsymbol{k})$ is taken into account since we only consider $z$-polarized light (along the nanotube axis) accounting for the depolarization effect that strongly suppresses light polarized perpendicular to the nanotube axis [15].

The time evolution of an operator $\hat{O}$ is calculated via Heisenberg equation of motion $i\hbar(\mathrm{d}/\mathrm{d}t)\hat{O} = [\hat{O}, H]$ with the Hamilton operator:

$$H = H_{0,\mathrm{c}} + H_{\mathrm{c-f}} + H_{\mathrm{c-c}}, \quad (2)$$

which determines the dynamics of a physical system, in particular the dynamics of the density matrix elements $\rho_{\boldsymbol{k}}^{\lambda\lambda'}(t)$ and $p_{\boldsymbol{k}}(t)$. The first two terms in Eq. (2) describe the non-interacting carrier system in the presence of the external electromagnetic field. In this work, a semiclassical approach is applied, i.e., the charge carriers are treated quantum mechanically, while the field is considered to be classical. Applying the formalism of the second quantization, the free carrier part $H_{0,\mathrm{c}}$ can be expressed as $H_{0,\mathrm{c}} = \sum_l \varepsilon_l a_l^+ a_l$ with the compound index $l = (\lambda, \boldsymbol{k})$. Within the $\boldsymbol{p}\cdot\boldsymbol{A}$ approach [16] the carrier–field interaction reads:

$$H_{\mathrm{c-f}} = i\frac{e_0\hbar}{m_0}\sum_{l,l'}\boldsymbol{M}_{l,l'}\cdot\boldsymbol{A}(t)a_l^+ a_{l'} \quad (3)$$

with the optical matrix elements:

$$\boldsymbol{M}_{l,l'} = \int \mathrm{d}\boldsymbol{r}\,\Phi_l^*(\boldsymbol{r})\nabla\Phi_{l'}(\boldsymbol{r}). \quad (4)$$

The third contribution of the Hamilton operator in Eq. (2) is given by the carrier–carrier interaction:

$$H_{\mathrm{c-c}} = \frac{1}{2}\sum_{l_1,l_2,l_3,l_4}V_{l_3,l_4}^{l_1,l_2}a_{l_1}^+ a_{l_2}^+ a_{l_4} a_{l_3} \quad (5)$$

with the Coulomb matrix elements:

$$V_{l_3,l_4}^{l_1,l_2} = \iint \mathrm{d}\boldsymbol{r}\,\mathrm{d}\boldsymbol{r}'\,\Phi_{l_1}^*(\boldsymbol{r})\Phi_{l_2}^*(\boldsymbol{r}')V(\boldsymbol{r}-\boldsymbol{r}')\Phi_{l_3}(\boldsymbol{r}')\Phi_{l_4}(\boldsymbol{r}),$$
$$(6)$$

where $V(\boldsymbol{r}-\boldsymbol{r}')$ is the screened Coulomb potential. The Coulomb interaction in one-dimensional structures needs to be treated with care [17]. The occurring problem of an infinite energy can be avoided by introducing a regularized Coulomb potential that takes into account that CNTs are not strictly one-dimensional. In this work, we use the Ohno potential which has already been shown to be a good approximation for CNTs [9, 11, 18]. Electron–phonon interaction is beyond the scope of this work, it can, however, be included into our model in a straightforward way [19].

The density matrix theory is based on Bloch equations [20] describing the temporal dynamics of charge carrier occupation $\rho_{\boldsymbol{k}}^{\lambda\lambda'}$ and the microscopic polarization $p_{\boldsymbol{k}}$:

$$\dot{p}_{\boldsymbol{k}}(t) = -i\omega_{\boldsymbol{k}}p_{\boldsymbol{k}}(t) - i\Omega(t)[\rho_{\boldsymbol{k}}^{cc}(t) - \rho_{\boldsymbol{k}}^{vv}(t)] + p_{\boldsymbol{k}}|_{\mathrm{scat}}, \quad (7)$$

$$\dot{\rho}_{\boldsymbol{k}}^{\lambda\lambda'}(t) = 2\,\mathrm{Im}[\Omega^*(t)p_{\boldsymbol{k}}(t)] + \rho_{\boldsymbol{k}}^{\lambda\lambda'}|_{\mathrm{scat}} \quad (8)$$

with $\lambda, \lambda' = (c, v)$ labeling the conduction and valence band, respectively. Due to the boundary condition for CNTs as rolled-up graphene layers, the two-dimensional wave vector $\boldsymbol{k} = (k_z, k_\perp)$ contains a continuous component $k_z$ along the nanotube axis and the quantized component $k_\perp = (2/d)m$ with the diameter $d$ and the subband index $m$ [1]. The Rabi frequency $\Omega(t)$ in Eqs. (7) and (8) describes the strength of the electron–light interaction including the influence of Coulomb effects. The band gap energy $\omega_{\boldsymbol{k}}$ determines the position of peaks in a linear spectrum. It already contains the renormalization due to the electron–electron interaction [13, 21].

In Section 3, we focus on linear optical spectra. Here, the Bloch Eqs. (7) and (8) are solved on the Hartree–Fock level neglecting scattering contributions. We include a phenomenologic parameter $\gamma$ into Eq. (7) to describe dephasing resulting from electron–phonon or other interactions. Its value determines the linewidth in the calculated spectra and is taken in this work to be $\gamma = (0.0125/\hbar)\,\mathrm{eV}$ [22]. In Section 4, we go beyond the Hartree–Fock level taking explicitly the scattering terms $p_{\boldsymbol{k}}(t)|_{\mathrm{scat}}$ and $\rho_{\boldsymbol{k}}^{\lambda\lambda'}(t)|_{\mathrm{scat}}$ into account. We treat the Coulomb interaction up to the second order Born approximation [20, 23]. Since we are interested in describing ultrafast carrier dynamics on short timescales, we also consider memory effects, i.e., we treat the correlations in a non-Markovian approach [20]. The scattering contributions in Eqs. (7) and (8) are determined by:

$$\dot{p}_{\boldsymbol{k}}(t)|_{\mathrm{scat}} \propto \sum_{\boldsymbol{q},\boldsymbol{k}'}V(\boldsymbol{k}',\boldsymbol{q},\boldsymbol{k})C_{\boldsymbol{k}',\boldsymbol{q},\boldsymbol{k}}(t) \quad (9)$$

with the Coulomb matrix element $V(\boldsymbol{k}',\boldsymbol{q},\boldsymbol{k})$ and the correlation function $C_{\boldsymbol{k}',\boldsymbol{q},\boldsymbol{k}}(t) = \langle a_{\boldsymbol{k}+\boldsymbol{q}}^+ a_{\boldsymbol{k}'}^+ a_{\boldsymbol{k}} a_{\boldsymbol{k}+\boldsymbol{q}}\rangle(t)$. The many-particle contribution couples the dynamics of single-particle elements of the density matrix to higher-order correlation terms: the dynamics of two-operator quantities couples to four-operator terms, the latter couple to six-operator terms, etc. This hierarchy problem is common in many-particle physics. In this work, the method of correlation expansion [24] is applied to truncate the hierarchy at the second order, i.e., only the dynamics of the four-operator correlations is taken into account. Applying again the Heisenberg equation and the Hamiltonian from Eq. (2), we find the correlation functions to be driven by nonlinear contributions, such as:

$$\frac{\mathrm{d}}{\mathrm{d}t}C_{\boldsymbol{k}',\boldsymbol{q},\boldsymbol{k}}(t) \propto (\rho_{\boldsymbol{k}'}(t) - \rho_{\boldsymbol{k}'+\boldsymbol{q}}(t))p_{\boldsymbol{k}}(t)p_{\boldsymbol{k}+\boldsymbol{q}}(t). \quad (10)$$

A detailed theory on non-equilibrium dynamics in CNTs is presented elsewhere [25].

**3 Linear optical spectra** After solving the Bloch equations (7) and (8), absorption spectra of nanotubes of arbitrary chiral angle and diameter can be calculated. The limit of our model is only given by the first-neighbor tight binding approximation. Figure 1 shows the absorption spectrum of the exemplary (10,0) zigzag nanotube. The three energetically lowest transitions $E_{11}$, $E_{22}$, and $E_{33}$ are shown. The dashed red line illustrates the free particle peaks renormalized by the repulsive electron–electron interaction. The occurring Van Hove singularities are typical for one-dimensional structures. The full blue line shows the same spectra, but including excitonic effects. Due to the attractive electron–hole coupling, bound electron–hole pairs are formed, which are characterized by symmetric Lorentzians. The spectrum reveals besides the exciton ground state also a series of excited states around the continuum edge. They become more pronounced at higher transitions.

The excitonic binding energy $E_b$ is in the range of 1 eV and can be easily determined as the difference between the excitonic Lorentzians and the corresponding free particle Van Hove singularities (see arrows in Fig. 1). The large binding energies are in good agreement with *ab initio* calculations [22, 26]. They can be ascribed to the relatively weak screening in CNTs, which are hollow cylinders. In particular, the higher transitions $E_{22}$ and $E_{33}$ show larger binding energies than $E_{11}$. Furthermore, the spectral weight is almost completely transferred from the continuum to the excitonic excitation. The free band-edge can still be seen in the excitonic spectrum, however, it is largely suppressed.

In addition to the established methods of optical spectroscopy, Rayleigh scattering has emerged as a characterization technique for individual single-walled CNTs [6,
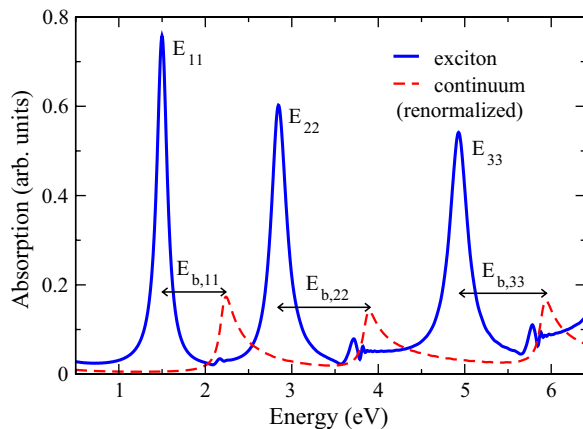
27] offering rapid data collection for both semiconducting and metallic tubes. Our approach also allows the calculation of Rayleigh scattering cross-section $\sigma(\omega) \propto |\chi(\omega)|^2$ for arbitrary CNTs [28, 29]. In particular, since $\sigma(\omega)$ is given by the full dielectric response, the real part of the optical susceptibility has an influence on the peak shape leading to characteristic features in Rayleigh spectra (not shown here).

**3.1 Environmental influence** The surrounding medium created by solvents and adsorbed molecules has a considerable influence on the optical properties of CNTs [7–12]. Here, we focus on a simple, widely used method [9–11] of considering the environmental effects by phenomenologically incorporating a dielectric background constant $\varepsilon_{bg}$ into the theory:

$$V(q) \rightarrow W(q) \equiv \frac{V(q)}{\varepsilon_{bg}}, \tag{11}$$

which describes an effective screening of the Coulomb potential. A more advanced study has been recently published integrating also the diameter dependence into $\varepsilon_{bg}$ [12]. Our aim is to show the basic influence of the surrounding material to semiconducting nanotubes. The internal dynamical screening (cp. Lindhard equation [20]), which is important for metallic nanotubes, is neglected. The introduction of the screened Coulomb potential $W(q)$ from Eq. (11) leads to changes in both the renormalization of the bandgap due to the repulsive electron–electron interaction as well as in the formation of excitons due to the attractive electron–hole coupling. As a result, the dielectric background constant has an influence on both the transition energies $E_{ii}$ as well as on the excitonic binding energies $E_{b,ii}$. Figure 2 illustrates the importance of the external screening for the excitonic binding energies for the three lowest transitions of the (10,0) tube. For a better insight into the functional dependence for both small and large $\varepsilon_{bg}$, the plot shows values up to $\varepsilon_{bg} = 10$. Increasing $\varepsilon_{bg}$ from 1 to 2 already leads to a considerable reduction of $E_{b,ii}$ to 0.3–0.5 eV, which is in good agreement with experimental results performed on nanotubes in an SDS medium [30, 31]. However, the exact value for the dielectric background constant in the SDS medium is difficult to determine, since it depends on the largely unknown coverage of the nanotube with the surfactant [7, 32]. The considerable reduction of $E_{b,ii}$ is a sign for a strongly suppressed electron–hole coupling due to the surrounding solvent. We also find a simple scaling law for the binding energies in dependence on $\varepsilon_{bg}$:

$$E_{b,ii} \propto A \varepsilon_{bg}^{-\beta_0} \tag{12}$$

with $\beta_0 \approx 1.3$ for all considered transitions $E_{ii}$, diameters $d$, and chiral angles $\phi$. The scaling law is valid for all nanotubes $(n_1, n_2)$. The coefficient $A$ varies with the transition $E_{ii}$ and the diameter $d$. A similar scaling law has also been found within the Bethe–Salpeter approach by



**Figure 1** (online color at: www.pss-b.com) Optical absorption spectrum of the (10,0) zigzag nanotube. The energetically lowest three transitions are shown. The blue solid line illustrates the spectrum containing excitonic effects, while the dashed red line shows the free particle spectrum, which already includes the renormalization due to the electron–electron coupling. The arrows indicate the corresponding excitonic binding energies.

Phys. Status Solidi B **246**, No. 11–12 (2009)
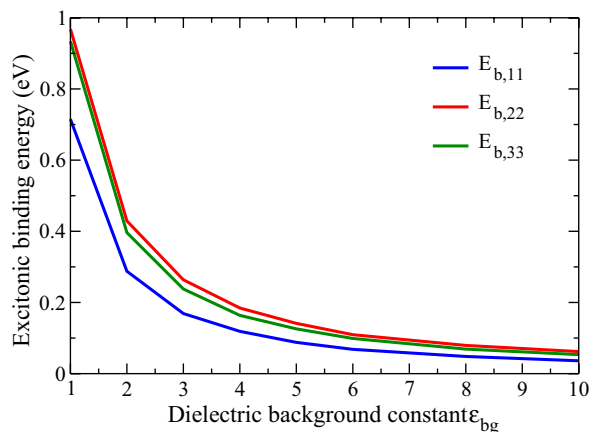
2595

**Original**

**Paper**

**Figure 2** (online color at: www.pss-b.com) Excitonic binding energies for the first three transitions of the exemplary (10, 0) zigzag nanotube are plotted as a function of the dielectric background constant $\varepsilon_{bg}$. The figure illustrates the influence of the surrounding medium on excitonic properties of carbon nanotubes.

Perebeinos et al. [11] and Capaz et al. [10] with a slightly different parameter $\beta_0 = 1.4$.

Figure 3 shows the influence of the external screening on the excitation position. In experimental studies, a red-shift by approximately 20–90 meV for tubes in a SDS medium compared to measurements in air ($\varepsilon_{bg} \approx 1$) has been observed [8, 32–37]. In theory, we also find a general decrease of the transition energy with increasing dielectric background constant $\varepsilon_{bg}$. The theory predicts a red-shift in the range of 0.1–0.2 eV already for $\varepsilon_{bg} = 2$, which is larger than in the experiment. A direct comparison, however, is difficult, since the dielectric background constant is not
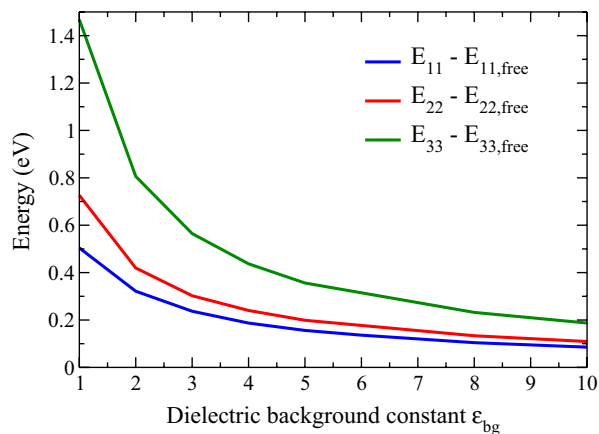


**Figure 3** (online color at: www.pss-b.com) The excitation energies of the first three transitions of the exemplary (10,0) zigzag nanotube are plotted as a function of the dielectric background constant $\varepsilon_{bg}$. For reasons of a better comparison between different transitions, we shifted the excitation energies by the value of the corresponding free particle energies with $E_{11,\text{free}} = 1.00\,\text{eV}$, $E_{22,\text{free}} = 2.18\,\text{eV}$, and $E_{33,\text{free}} = 3.52\,\text{eV}$.

known for the used solvents. For peak positions, we find a different behavior for small and high $\varepsilon_{bg}$ yielding the following scaling law:

$$\Delta E_{ii} \propto B \exp(-\beta_1 \varepsilon_{bg}) + C\varepsilon_{bg}^{-\beta_2} \tag{13}$$

with $\beta_1 \approx 0.2$, $\beta_2 \approx 0.8$. The parameters $B$ and $C$ vary with the diameter $d$ and the transition $E_{ii}$, but the functional dependence on the dielectric background constant remains the same.

**4 Relaxation dynamics** The description of ultrafast intrasubband carrier relaxation processes requires an extension of the theory beyond the Hartree–Fock level. The scattering contributions $p_k|_{\text{scat}}$ and $\rho_k^{cc,v}|_{\text{scat}}$ in Eqs. (7) and (8) need to be calculated microscopically. In Section 2, their dynamics is shown to be driven by Coulomb correlations functions $C_{k',q,k}(t)$. The evaluation of the Bloch equations (7) and (8) including explicitly the dynamics of $C_{k',q,k}(t)$ yields insight into nonlinear regime of intrasubband carrier relaxation as well as into the optical dephasing. For numerical reasons, we restrict our consideration to a two-band model.

Figure 4 shows the carrier dynamics as a function of the wave vector $k_z$ along the nanotube axis and time. The carriers are optically excited at 2 eV, which is energetically far above the excitonic resonance. The excitation field is described by the linearly polarized vector potential $A(t)$ with a Gaussian pulse with the amplitude $A_0 = 0.13\,\text{eV fs}\,(e_0\,\text{nm})$ and the FWHM $\sigma = 65\,\text{fs}$. In the first femtoseconds, a non-equilibrium occupation is built. After the excitation pulse is switched off, the carriers equilibrate from the non-equilibrium into a Fermi-like distribution on the femtosecond time scale. The occurring oscillations of the electron plasma reflecting the energy–time uncertainty principle are typical features for a non-Markovian dynamics [38]. The chiral angle is found to have a negligible influence on the relaxation time. In contrast, the diameter plays an important role, since the strength of the Coulomb driven scattering processes is sensitive to the diameter of the tube.

Furthermore, for strong excitations at the excitonic resonance, we find excitation induced dephasing of the excitonic polarization (not shown here) [39, 40].
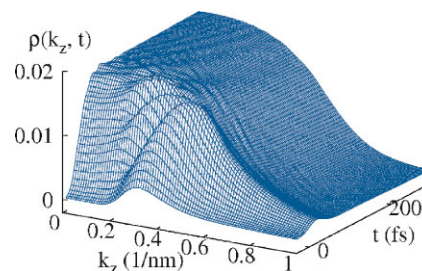


**Figure 4** (online color at: www.pss-b.com) Carrier dynamics in the exemplary (11,6) semiconducting nanotube after excitation above the excitonic resonance.
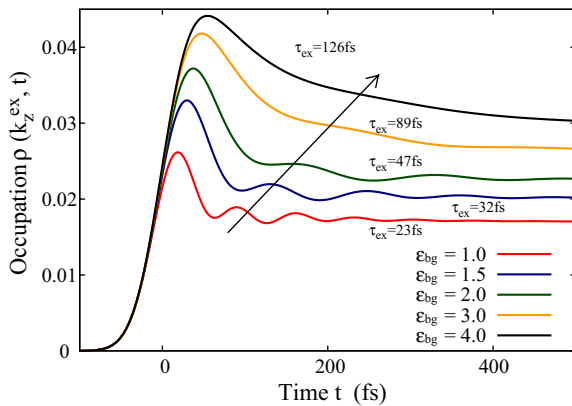
**Figure 5** (online color at: www.pss-b.com) Carrier relaxation in the exemplary (11, 6) semiconducting nanotube for different dielectric background constants $\varepsilon_{bg}$. The higher $\varepsilon_{bg}$, i.e., the larger the external screening, the slower is the relaxation dynamics and the less pronounced are the plasma oscillations.

**4.1 Environmental influence** The effective screening of the Coulomb potential due to the surrounding medium does not only influence linear properties. We also find a considerable effect on the non-equilibrium relaxation dynamics. Figure 5 shows the relaxation of optically excited electrons as a function of time for different dielectric background constants $\varepsilon_{bg}$. The wave vector is fixed to $k_z^{ex}$ corresponding to the excitation position. The relaxation times $\tau_{ex}$ are obtained from an exponential fit at the carrier occupation maximum. Surprisingly, we find an approximately linear relation between $\varepsilon_{bg}$ and $\tau_{ex}$: the higher the external screening, the weaker the Coulomb interaction, the less efficient are the Coulomb driven scattering processes and the longer is the relaxation time $\tau_{ex}$. In a simple hand waving argument, one would expect $\tau_{ex} \propto \varepsilon_{bg}^2$, since the scattering contributions are proportional to $W^2$ [23]. However, the strongly nonlinear Coulomb correlation functions also show a complex dependence on the occupation probability $\rho_k(t)$ and on the microscopic polarization $p_k(t)$.

**5 Conclusions** We have presented microscopic calculations on the importance of the surrounding medium for optical properties of CNTs. In particular, we have discussed its influence on the excitation positions, excitonic binding energies, and the relaxation times. In agreement with experimental studies, we find a considerable red-shift of the excitonic peaks in dependence of the dielectric background constant $\varepsilon_{bg}$. Due to the reduced electron–hole coupling, the excitonic binding energies are strongly reduced. Furthermore, the effective screening of the Coulomb potential slows down the relaxation dynamics of optically excited carriers in CNTs. More advanced studies including the energy dependence of the dielectric screening are necessary to obtain a better understanding of environmental effects.

## References

[1] S. Reich, C. Thomsen, and J. Maultzsch, Carbon Nanotubes: Basic Concepts and Physical Properties (Wiley-VCH, Berlin, 2004).

[2] A. Jorio, M. Dresselhaus, and G. Dresselhaus, Carbon Nanotubes: Advanced Topics in the Synthesis, Structure, Properties and Applications (Springer, Heidelberg, Germany, 2008).

[3] S. M. Bachilo, M. S. Strano, C. Kittrell, R. H. Hauge, R. E. Smalley, and R. B. Weisman, Science **298**, 2361 (2002).

[4] Y. Miyauchi, S. Chiashi, Y. Murakami, Y. Hayashida, and S. Maruyama, Chem. Phys. Lett. **387**, 198 (2004).

[5] H. Telg, J. Maultzsch, S. Reich, F. Hennrich, and C. Thomsen, Phys. Rev. Lett. **93**, 177401 (2004).

[6] M. Y. Sfeir, F. Wang, L. Huang, C. Chuang, J. Hone, S. P. O'Brien, T. F. Heinz, and L. E. Brus, Science **306**, 1540 (2004).

[7] J. Choi and M. S. Strano, Appl. Phys. Lett. **90**(22), 223114 (2007).

[8] O. Kiowski, S. Lebedkin, F. Hennrich, S. Malik, H. Rosner, K. Arnold, C. Surgers, and M. M. Kappes, Phys. Rev. B **75**(7), 075421 (2007).

[9] J. Jiang, R. Saito, G. G. Samsonidze, A. Jorio, S. G. Chou, G. Dresselhaus, and M. S. Dresselhaus, Phys. Rev. B **75**(3), 035407 (2007).

[10] R. B. Capaz, C. D. Spataru, S. Ismail-Beigi, and S. G. Louie, Phys. Rev. B **74**(12), 121401 (2006).

[11] V. Perebeinos, J. Tersoff, and P. Avouris, Phys. Rev. Lett. **92**, 257402 (2004).

[12] Y. Miyauchiand, R. Saito, K. Sato, Y. Ohno, S. Iwasaki, T. Mizutani, J. Jiang, and S. Maruyama, Chem. Phys. Lett. **442**, 394 (2007).

[13] M. Hirtschulz, F. Milde, E. Malić, S. Butscher, C. Thomsen, S. Reich, and A. Knorr, Phys. Rev. B **77**(3), 035403 (2008).

[14] E. Malić, M. Hirtschulz, F. Milde, A. Knorr, and S. Reich, Phys. Rev. B **74**(19), 195431 (2006).

[15] H. Ajiki and T. Ando, J. Phys. Soc. Jpn. **62**, 4267 (1993).

[16] M. O. Scully and M. S. Zubairy, Quantum Optics (Cambridge University Press, Cambridge, UK, 1997).

[17] R. Loudon, Am. J. Phys. **27**, 649 (1959).

[18] H. Zhao and S. Mazumdar, Phys. Rev. Lett. **93**, 157402 (2005).

[19] S. Butscher, F. Milde, M. Hirtschulz, E. Malić, and A. Knorr, Appl. Phys. Lett. **91**(20), 203103 (2007).

[20] H. Haug and S. W. Koch, Quantum Theory of the Optical and Electronic Properties of Semiconductors (World Scientific, Singapore, 2004).

[21] E. Malić, M. Hirtschulz, F. Milde, J. Maultzsch, S. Reich, and A. Knorr, Phys. Status Solidi B **245**, 2155 (2008).

[22] C. D. Spataru, S. Ismail-Beigi, L. X. Benedict, and S. G. Louie, Phys. Rev. Lett. **92**, 077402 (2004).

[23] M. Hirtschulz, F. Milde, E. Malić, C. Thomsen, S. Reich, and A. Knorr, Phys. Status Solidi B **245**, 2164 (2008).

[24] J. Fricke, Ann. Phys. **252**(142), 478–498 (1996).

[25] M. Hirtschulz, E. Malić, F. Milde, and A. Knorr, Phys. Rev. B **80**(8), 085405 (2009).

Phys. Status Solidi B **246**, No. 11–12 (2009)

2597

[26] E. Chang, G. Bussi, A. Ruini, and E. Molinari, Phys. Rev. B **72**(19), 195423 (2005).

[27] Y. Wu, J. Maultzsch, E. Knoesel, B. Chandra, M. Y. Huang, M. Y. Sfeir, L. E. Brus, J. Hone, and T. F. Heinz, Phys. Rev. Lett. **99**(2), 027402 (2007).

[28] E. Malić, M. Hirtschulz, F. Milde, Y. Wu, J. Maultzsch, T. F. Heinz, A. Knorr, and S. Reich, Phys. Rev. B **77**(4), 045432 (2008).

[29] E. Malić, M. Hirtschulz, F. Milde, Y. Wu, J. Maultzsch, T. F. Heinz, A. Knorr, and S. Reich, Phys. Status Solidi B **244**(11), 4240 (2007).

[30] J. Maultzsch, R. Pomraenke, S. Reich, E. Chang, D. Prezzi, A. Ruini, E. Molinari, M. S. Strano, C. Thomsen, and C. Lienau, Phys. Rev. B **72**, 241402(R) (2005).

[31] F. Wang, G. Dukovic, L. E. Brus, and T. F. Heinz, Science **308**, 838 (2005).

[32] M. Strano, V. C. Moore, M. K. Miller, M. J. Allen, E. H. Haroz, C. Kittrell, R. H. Hauge, and R. E. Smalley, J. Nanosci. Nanotechnol. **3**(1), 81–86 (2003).

[33] V. Moore, M. S. Strano, E. H. Haroz, R. H. Hauge, R. E. Smalley, J. Schmidt, and Y. Talmon, Nano Lett. **3**(10), 1379–1382 (2003).

[34] J. Lefebvre, J. M. Fraser, Y. Homma, and P. Finnie, Appl. Phys. A **78**(8), 1107–1110 (2004).

[35] T. Okazaki, T. Saito, K. Matsuura, S. Ohshima, M. Yumura, and S. Iijima, Nano Lett. **5**(12), 2618–2623 (2005).

[36] Y. Ohno, S. Iwasaki, Y. Murakami, S. Kishimoto, S. Maruyama, and T. Mizutani, Phys. Rev. B **73**(23), 235427 (2006).

[37] A. G. Walsh, A. N. Vamivakas, Y. Yin, S. B. Cronin, M. S. Unlu, B. B. Goldberg, and A. K. Swan, Nano Lett. **7**(6), 1485 (2007).

[38] H. Haug and A. Jauho, Quantum Kinetics in Transport and Optics of Semiconductors (Springer Verlag, Berlin, 2007).

[39] M. Kira and S. Koch, Prog. Quantum Electron. **30**(5), 155 (2006).

[40] E. Malić, M. Hirtschulz, S. Reich, and A. Knorr, Phys. Status Solidi RRL **3**, 196 (2009).